

HD 65949: Rosetta stone or red herring[★]

C. R. Cowley,^{1†} S. Hubrig,² P. Palmeri,³ P. Quinet,^{3,4} É. Biémont,^{3,4}
G. M. Wahlgren,^{5,6} O. Schütz⁷ and J. F. González⁸

¹Department of Astronomy, University of Michigan, Ann Arbor, MI 48109-1042, USA

²Astrophysikalisches Institut Potsdam, An der Sternwarte 16, 14482 Potsdam, Germany

³Astrophysique et Spectroscopie, Université de Mons-UMONS, B-7000 Mons, Belgium

⁴IPNAS, Université de Liège, Sart Tilman B15, B-4000 Liège, Belgium

⁵Catholic University of America, 620 Michigan Avenue NE, Washington, DC 20064, USA

⁶NASA Goddard Space Flight Center, Code 667, Greenbelt, MD 20771, USA

⁷European Southern Observatory, Casilla 19001, Santiago 19, Chile

⁸Instituto de Ciencias Astronómicas, de la Tierra y del Espacio, Casilla 49, 5400 San Juan, Argentina

Accepted 2010 February 15. Received 2010 February 15; in original form 2009 November 26

ABSTRACT

HD 65949 is a late B star with exceptionally strong Hg II λ 3984, but it is not a typical HgMn star. The Re II spectrum is of extraordinary strength. Abundances or upper limits are derived here for 58 elements based on a model with $T_{\text{eff}} = 13\,100\text{ K}$ and $\log(g) = 4.0$. Even- Z elements through nickel show minor deviations from solar abundances. Anomalies among the odd- Z elements through copper are mostly small. Beyond the iron peak, a huge scatter is found. Enormous enhancements are found for the elements rhenium through mercury ($Z = 75\text{--}80$). We note the presence of Th III in the spectrum. The abundance pattern of the heaviest elements resembles the $N = 126$ r-process peak of solar material, though not in detail. An odd- Z anomaly appears at the triplet (Zr Nb Mo), and there is a large abundance jump between Xe ($Z = 54$) and Ba ($Z = 56$). These are signatures of chemical fractionation.

We find a significant correlation of the abundance excesses with second ionization potentials for elements with $Z > 30$. If this is not a red herring (false lead), it indicates the relevance of photospheric or near-photospheric processes. Large excesses (4–6 dex) require diffusion from deeper layers with the elements passing through a number of ionization stages. That would make the correlation with second ionization potential puzzling. We explore a model with mass accretion of exotic material followed by the more commonly accepted differentiation by diffusion. That model leads to a number of predictions which challenge future work.

New observations confirm the orbital elements of Giesecking and Karimie, apart from the systemic velocity, which has increased. Likely primary and secondary masses are near 3.3 and 1.6 M_{\odot} , with a separation of ca. 0.25 au.

New atomic structure calculations are presented in two appendices. These include partition functions for the first through third spectra of Ru, Re and Os, as well as oscillator strengths in the Re II spectrum.

Key words: astrochemistry – diffusion – stars: abundances – stars: chemically peculiar – stars: individual: HD 65949 – stars: individual: HR 7143.

1 TOWARDS AN UNDERSTANDING OF CHEMICALLY PECULIAR STARS

In situ chemical separation, under gravitational and radiative forces, is accepted as the basic explanation of abundance anomalies in upper main-sequence, chemically peculiar (CP) stars. Nevertheless, there have been few breakthroughs of the stature of arguments originally posed by Michaud (1970). Briefly, these were that the anomalies appeared in the stable atmospheres of slowly rotating stars with radiative envelopes. Additionally, the more abundant elements,

[★]Based on observations obtained at the European Southern Observatory, Paranal and La Silla, Chile [ESO programmes 076.D-0172(A) and 081.D-0498(A)], HARPS data obtained during engineering nights and at the Complejo Astronómico El Leoncito.

†E-mail: cowley@umich.edu

helium, carbon, nitrogen and oxygen could have little radiative support because their strong lines would be saturated. Time has not dimmed the relevance of that insight.

Scientific breakthroughs often hinge on the location of special cases, where the effects under consideration are large. A code breaker is at a severe disadvantage when faced with a brief message. With a long message, it is more likely that the regularities of a language will lead to a decryption key. We hope that this paper represents a kind of longer message, and can serve as a Rosetta stone, for an understanding of the more bizarre anomalies seen in CP stars. We provide information on more elements (58) than in a typical study of similar stars (20–30). Additionally, the number of anomalies is very large.

The extensive analysis of Castelli & Hubrig (2004, hereafter CH04) provides a guide for this paper. Their study of the classical HgMn star, HR 7143 (HD 175640), reported abundances for 40 elements. The abundance anomalies are similar in some ways to those of HD 65949, and dissimilar in others. It has been helpful to compare results for the two stars. A detailed comparison with HR 7143 has been possible because of the spectra posted on the web site of Castelli (2009).

The HgMn star χ Lup has also been the subject of intensive study (cf. Wahlgren 2005, and many cited references therein). The star is significantly cooler ($T_{\text{eff}} = 10\,650$ K) than HD 65949 (ca. 13 100 K), and many important results were obtained from *Hubble Space Telescope* (HST) observations for which there is no comparable material for HD 65949. We briefly discuss the χ Lup abundances in the light of this paper.

2 AN UNUSUAL LATE B SPECTRUM

Abt & Morgan (1969) noted the great strength of Hg II $\lambda 3984$ in the spectrum of HD 65949, and remarked that it did not seem to be an HgMn star. Hubrig et al. (2006) reported a weak magnetic field which might indicate a relation to the magnetic sequence of CP stars (Preston 1974).

More recent high-resolution European Southern Observatory (ESO) observations revealed a truly unusual spectrum (Cowley et al. 2006, hereafter Paper I; Cowley, Hubrig & Wahlgren 2008, hereafter Paper II). In addition to the possibly record-setting strength of Hg II $\lambda 3984$, along with strong Pt II lines of Os II and especially Re II were numerous. Osmium and rhenium have been investigated in the ultraviolet (UV) spectrum of χ Lup (Wahlgren et al. 1997; Ivarsson et al. 2004), but the presence of lines of these elements in ground-based spectra is unusual.

The richness of the line spectrum is due not only to the unusual abundances. The lines are extremely sharp. We estimate from spectral synthesis that $v \sin i = 0.5 \pm 0.5$ km s⁻¹.

This paper is a more complete abundance analysis of HD 65949, though based primarily on equivalent widths. For rich spectra, such as Fe I and Fe II, we obtained, hopefully, a sufficient number of measurements, but did not attempt to analyse all possibly relevant features. In this respect, the CH04 work is undoubtedly superior since the entire spectrum of HR 7143 was synthesized. However, relatively small errors in the present analysis are less important than they might otherwise be, given the large departures of many values from the standard (solar) abundance distribution (e.g. Asplund et al. 2009).

HD 65949 is located in the young cluster NGC 2516, which is known for more than a typical number of CP stars. This cluster also has an unusual number of X-ray sources (Wolk et al. 2004). These facts make it tempting to suggest that mass transfer might be

relevant for some aspect of the anomalies. This is an old idea, which Wahlgren et al. (1995) remarked ‘remains a distant alternative, but possibly a collaborator to diffusion theory’.

3 THE ATMOSPHERE OF HD 65949

The effective temperature of HD 65949 is uncertain by several hundred degrees. The estimate used in Paper I, $T_{\text{eff}} = 13\,600$ K, came from averaged Strömgren and H β photometry (Hauck & Mermilliod 1998), and the calibration of Moon & Dworetzky (1985) and implemented by Moon (1984). We used a version of the Moon code kindly supplied by Dr B. Smalley. For Paper II, we adopted a temperature 1000 K lower, which gave equal abundances for Fe I, Fe II and Fe III. Here, the reasoning was that for abundances it is more important to have the ionization correct than the colour temperature. Since that work, we have become more convinced of the plausible relevance of stratification in the atmospheres of early stars. When an element is non-uniformly distributed in a photosphere, the apparent ionization temperature of one element will not in general indicate the correct degree of ionization of another.

A computer code kindly supplied by Dr P. North (cf. Kunzli et al. 1997) allows one to include an abundance estimate in the calculation of T_{eff} and $\log(g)$. Geneva photometry was obtained from the online General Catalogue of Photometric Data of Mermilliod, Hauck & Mermilliod (2007). The code requires a reddening estimate, which we obtained from measurements of the interstellar Na I D₂ and K I resonance lines, with the help of the calibration of Munari & Zwitter (1997). We adopted $E(B - V) = 0.042$ (smaller than typical measurements for NGC 2516, ca. 0.1; cf. references in van Leeuwen 2009). Conversions of reddening from the *UBV* system they used to the Geneva system were taken from Paunzen, Schnell & Maitzen (2006). Dr North’s code calculates T_{eff} and $\log(g)$ for [Fe/H] values of -1, 0 and +1. We averaged the results for 0 and +1, and obtained the adopted value $T_{\text{eff}} = 13\,100$ K. This value is conveniently between that obtained from Strömgren photometry and that giving iron ionization equilibrium.

Dr North’s code also gives surface gravity: $\log(g) = 4.2$. However, our calculations were all made with $\log(g) = 4.0$. Low Balmer profiles are relatively insensitive to the effective temperatures considered here, but agree well with the assumed $\log(g) = 4.0$ (Fig. 1).

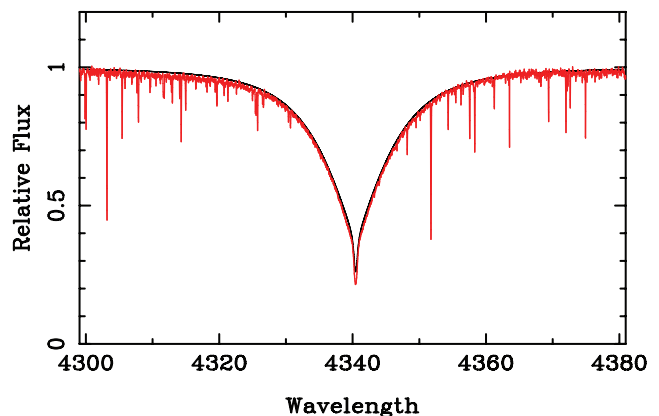


Figure 1. H γ profile for $T_{\text{eff}} = 13\,100$ K, $\log(g) = 4.0$. The calculated profile is nearly obscured by the observations (grey, red in online version). The HD 65949 profile is from a HARPS (Mayor et al. 2003) spectrum obtained on 2009 March 31. No metal lines were included in the calculation.

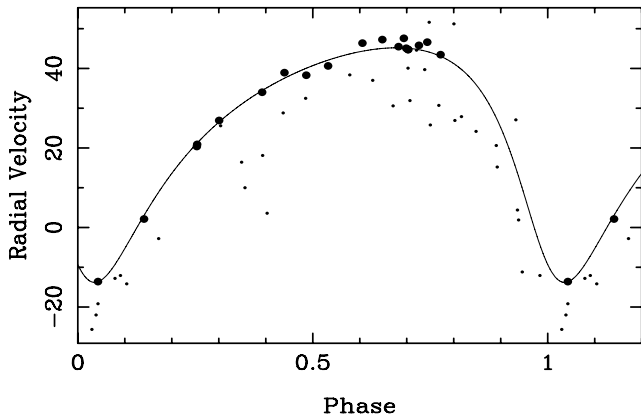


Figure 2. Old (dots) plus new (filled circles) radial velocities using orbital elements of Table 2. A closer fit to the new data may be obtained if the period is determined only from the new data. The current plot highlights the γ velocity difference between the old and new data.

No stratification was assumed in any of the abundance calculations.

4 SPECTRA

ESO/FEROS spectra are discussed in Kaufer et al. (1999). The useful coverage was $\lambda\lambda 3603\text{--}9211$, with a resolving power of 48 000. They were supplemented by a UVES (Dekker et al. 2000) spectrum obtained on 2008 August 4 ($\lambda\lambda 3258\text{--}4517$ and $5655\text{--}9464$). The resolving power in the blue arm is 80 000 and 110 000 in the red. Additionally, we used HARPS spectra obtained on 2008 December 14, 2009 March 31, 2009 June 2 and 2009 June 3. The wavelength coverage is $\lambda\lambda 3972\text{--}6911$, with a resolving power of 120 000. Most quantitative measurements were made on the 2008 December spectrum, where the signal-to-noise ratio was 120–150.

Most abundances are based on equivalent width measurements carried out with MICHIGAN software, which fit a Voigt profile to the stellar features. Equivalent widths for few hyperfine and helium profiles were obtained from quadrilaterals or triangles estimated to have the same area as the more complex absorption profiles.

5 BINARITY

HD 65949 was one of the objects investigated in NGC 2516 for binarity by Abt & Levy (1972). Their observations were combined with objective prism measurements by Giesecking (1978) and Giesecking & Karimie (1982), who found orbital elements very close to those adopted here (Table 2). We may group the radial velocities roughly into two time periods. The ‘old’ measurements were made within the interval from 1967 November through 1978 April. ‘New’ measurements followed some 20 yr later, from 1998 January to 2009 June. The newer measurements are clearly more precise, as shown in Fig. 2. This is expected, as many of the older measurements were made from objective prism spectra.

Table 1 gives the more recent, previously unpublished, radial velocities, plotted in Fig. 2. The ESO FEROS and UVES instruments are discussed in Section 4. The REOSC spectrograph is described by González & Lasset (2000), and Pintado & Adelman (2003) discuss the EBASIM instrument.

Even though the old measurements are less precise by a factor of 10–100, they are useful for the period calculation since they provide a time-base of about four decades. We performed a global

Table 1. New radial velocity measurements of HD 65949.

HJD–240 0000	Phase	V_r (km s ⁻¹)	Spectrograph
50835.6937	0.7901	45.80	REOSC
50836.6782	0.8363	43.50	REOSC
53663.8587	0.6686	46.38	FEROS
53664.7578	0.7109	47.26	FEROS
53665.7295	0.7565	47.57	FEROS
53666.7902	0.8064	46.65	FEROS
53890.4733	0.3159	20.34	REOSC
53890.4882	0.3166	20.91	REOSC
53891.4820	0.3633	26.92	REOSC
53893.4307	0.4549	34.05	EBASIM
53894.4388	0.5022	38.96	EBASIM
54462.7415	0.2034	2.10	REOSC
54682.9258	0.5485	38.32	UVES
54683.9155	0.5950	40.63	UVES
54814.8034	0.7446	45.48	HARPS
54907.6066	0.1049	-13.63	REOSC
54921.5702	0.7610	45.05	HARPS
54985.4926	0.7643	44.72	HARPS
54985.5149	0.7654	44.72	HARPS

Table 2. SB1 orbital elements and corresponding mass function, $f(m)$, for HD 65949. Elements other than the period use only recent data.

Element	Value	Error
V_γ (km s ⁻¹)	25.7	± 1.9
K_1 (km s ⁻¹)	29.5	± 1.4
ω (°)	148	± 7
e	0.40	± 0.05
P (d)	21.2836	± 0.0012
$f(m)$ (M_\odot)	0.0437	± 0.0067

fit of all the observations to determine the period. Then we kept the period fixed and fit the remaining parameters using only the new measurements. The resulting parameters are listed in Table 2.

The adopted $T_{\text{eff}} = 13\,100$ K, and a fit to the data of Torres, Andersen & Giménez (2010) then yields $M_V = -0.02$, for a main-sequence star. The corresponding mass is $\approx 3.3 M_\odot$. Since no absorption lines from the secondary are seen, we assume a flux ratio ≤ 0.1 , or $\Delta M_V > 2.5$. The calibration gives $M/M_\odot \approx 1.52$, for $M_V \approx 2.48$, commensurate with a mass ratio, $q < 0.5$, expected for main-sequence binary stars. If we fix the primary mass at $3.3 M_\odot$, the mass function, $f(m) = 0.0446$, yields a secondary mass between 1.52 and $0.92 M_\odot$ for inclinations in the range $41^\circ\text{--}90^\circ$. Smaller inclinations are less likely since they would lead to larger secondary masses. Masses of $3.3 M_\odot$ for the primary, and from 1.52 to $0.92 M_\odot$ for the secondary, give separations $a_1 + a_2$ from 0.254 to 0.243 au.

The binarity of the HD 65949 system is of interest in view of the suggestion made below that mass exchange may be relevant for the surface chemistry. We note the increase in the systemic velocity of the binary system, which appears convincing in spite of the larger scatter of the older measurements. Note also that there is a systematic difference of 2 km s⁻¹ between the FEROS and HARPS observations, taken at the same phase, but separated by 3.5 yr.

A fit of the centre-of-mass velocity, keeping all other orbital parameters fixed, gives $V_\gamma = 16.9 \pm 1.5$ and 25.7 ± 0.2 km s⁻¹ for the old and the new measurements, respectively. A third body is therefore suspected to account for the change in systemic velocity.

6 ATOMIC PARAMETERS

Most of the atomic lines used in this paper were sufficiently weak that damping parameters are not important. We used default Stark damping from Cowley (1971) and Unsöld (1955) formula for van der Waals damping, but enhanced by a factor of 2. Only the Ca II K-line and lines from the infrared triplet were strong enough that Stark damping began to be relevant. We used the parameters adopted by CH04.

Default oscillator strengths were from VALD (Kupka et al. 1999), but supplemented as noted in the element-by-element discussion in Appendix A. Special calculations of partition functions and oscillator strengths were made for this paper, as noted in the Appendices B and C.

For Cr II, Ti II and Mn II, we used VALD and Kurucz (1995) to retain only lines that were allowed by LS-coupling selection rules. All oscillator strengths for third spectra of the lanthanides were from the DREAM data base (Biémont, Palmeri & Quinet 1999).

7 ABUNDANCES

Table 3 lists abundances or upper limits for 58 elements listed in column 1. Logarithmic ratios of individual abundances to the total elemental abundances including hydrogen follow in column 2. Column 3 gives error estimates, which are usually the standard deviations of the results from the number of lines used shown in column 4. For a few elements, the error is the difference in determinations from two ionization stages. There is no entry for upper limits based on a single line, but we estimate an uncertainty of some 0.5 dex. The solar abundance from Asplund et al. (2009) is in column 5, while column 6 is the difference in the stellar and solar values.

The stellar abundances are plotted in Fig. 3, along with corresponding solar values. Generally small deviations from the solar pattern are seen, especially for the even- Z elements with Z less than about 30. Beyond this point, the stellar abundances scatter wildly, with excesses ranging up to 6 dex (Re and Hg).

8 NON-NUCLEAR SIGNATURES

The abundance pattern of Fig. 3 shows a number of features that indicate the influence of non-nuclear processes. Interestingly, all such indications are for elements with Z greater than about 30 (zinc). The most common non-nuclear pattern shown in late B CP stars is an abundance of Mn ($Z = 25$), greater than that of either Cr ($Z = 24$) or Fe ($Z = 26$). This has been called an *odd- Z anomaly* since nuclear processes do not make more of odd- Z elements relative their even- Z neighbours (Li, Be, B excepted). That anomaly at Mn is not seen in HD 65949, but does appear in the typical HgMn star HR 7143 (CH04).

Beyond the iron peak, there is often an odd- Z anomaly at yttrium ($Z = 39$), which can be more abundant than its even- Z neighbours, Sr and Zr (Guthrie 1971; Adelman et al. 2001). This anomaly is clearly present in HR 7143, but not in HD 65949. However, the next triplet containing an odd- Z element, Zr, Nb ($Z = 41$), Mo does form an odd- Z anomaly in HR 65949. CH04 do not report abundances for Nb and Mo. Indeed, abundances for these two elements are rarely (if ever) reported for HgMn or related (HR 6000, HR 6870) stars.

Just as significant as the odd- Z anomalies are two highly fractionated even- Z neighbours: Xe and Ba. We find Xe more abundant than Ba by 4.2 or more dex. None of the standard (r - or s -process) neutron addition schemes would produce so severe a fractionation. Note that a Xe–Ba fractionation of 3.31 dex occurs in HR 7143.

Table 3. Abundances in HD 65949, the Solar system, and their differences (see text). Results for individual ions may be found in Appendix A.

Element	$\log(N/N_{\text{tot}})$	$\pm(\text{s.d.})$	n	$[\log(N/N_{\text{tot}})]_{\odot}$	$[N]$
He	-1.95	0.14	8	-1.11	-0.84:
C	-3.67	0.40	2	-3.61	-0.06
N	≤ -6.52		1	-4.21	-2.31:
O	-3.24	0.16	9	-3.35	0.11:
Ne	-4.29	0.16	10	-4.11	-0.18
Na	-5.42	0.13	2	-5.80	0.38
Mg	-4.80	0.45	13	-4.44	-0.36
Al	-6.44	0.24	4	-5.59	-0.85
Si	-4.69	0.26	12	-4.53	-0.16
P	-5.13	0.29	19	-6.63	1.50
S	-4.92	0.24	34	-4.92	0.00
Cl	≤ -7.09		1	-6.54	≤ -0.55
Ar	≤ -6.07		1	-5.64	≤ -0.43 :
Ca	-5.81	0.53	8	-5.70	-0.11:
Sc	-8.18	0.07		-8.89	0.71
Ti	-6.89	0.28	54	-7.09	0.20
V	≤ -8.65		1	-8.11	≤ -0.54
Cr	-5.87	0.31	63	-6.40	0.53
Mn	-6.06	0.15	22	-6.61	0.55
Fe	-4.06	0.24	98	-4.54	0.48
Co	≤ -5.76			-7.05	≤ 1.29
Ni	-6.35	0.31	5	-5.82	-0.53
Cu	≤ -5.81		1	-7.85	≤ 2.04
Zn	≤ -7.8		1	-7.48	≤ -0.32
Ga	≤ -7.50		1	-9.00	≤ 1.50
Br	-6.81	0.50	3	-9.50	2.69
Kr	-5.85	0.13	5	-8.79	2.94
Rb	≤ -6.70		1	-9.52	≤ 2.82
Sr	-6.76	0.45	6	-9.17	2.41
Y	-7.66	0.11	14	-9.83	2.17
Zr	-7.90	0.17	3	-9.46	1.56
Nb	-7.26	0.29	22	-10.58	3.32
Mo	-7.86	0.34	4	-10.16	2.30
Ru	-6.50	0.48	20	-10.29	3.79
Rh	-7.43		1	-11.13	3.70
Pd	-5.84	0.14	4	-10.47	4.63
Cd	≤ -7.82		1	-10.33	≤ 2.51
Sn	≤ -8.42		1	-10.00	≤ 1.58
Xe	-5.42	0.11	6	-9.80	4.38
Cs	-7.50		1	-10.96	3.46
Ba	≤ -9.64		1	-9.86	0.22
Ce	≤ -9.79		1	-10.46	0.67
Pr	-8.31	0.21	16	-11.32	3.01
Nd	-8.03	0.32	12	-10.62	2.59
Eu	≤ -8.50		1	-11.52	≤ 3.02
Dy	-8.06	0.44	12	-10.94	2.88
Ho	-8.18	0.31	12	-11.56	3.38
Er	-8.80	0.21	3	-11.12	2.32
Yb	-8.69		1	-11.20	2.51
W	≤ -8.14		1	-11.19	≤ 3.05
Re	-5.81	0.27	32	-11.78	5.97
Os	-5.27	0.53	13	-10.64	5.37
Pt	-5.22	0.15	6	-10.42	5.20
Au	-6.96	0.52	3	-11.12	4.16
Hg	-4.59	0.29	4	-10.87	6.28
Pb	≤ -8.12		1	-10.29	≤ 2.17
Bi	≤ -8.00	0.50	2	-11.39	≤ 3.39
Th	-9.18	0.17	8	-12.02	2.84

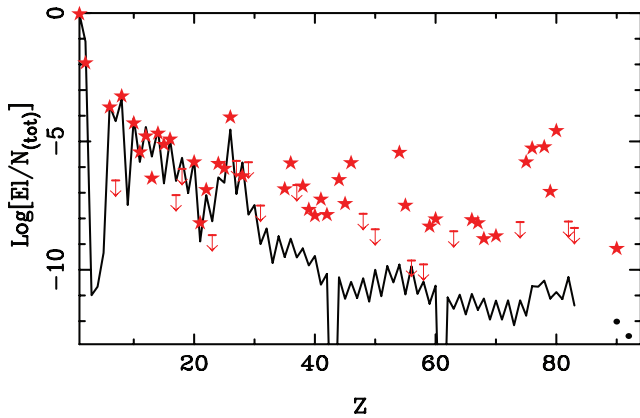


Figure 3. Solar (black line) and stellar (stars) abundances. Upper limits are indicated by horizontal lines with arrows pointing down. Solar points for uranium and thorium are filled circles.

Similar (or larger) values probably hold for other HgMn stars where Xe II has been identified. However, the Ba II lines are presumably not seen, and upper limits have not been computed.

9 LATE B STAR ABUNDANCES COMPARED

9.1 HD 65949 and HR 7143

Fig. 4 is similar to Fig. 3, but shows abundances of both HD 65949 and HR 7143 (CH04). Vertical lines connect elements with abundances available for both stars. Among the elements below zinc ($Z = 30$), the even- Z elements, especially the lighter ones, are not far from their solar values. Larger departures from the solar pattern are seen among the odd- Z elements. These are usually small or negative in HD 65949. A nitrogen ($Z = 7$) deficiency is a general characteristic of HgMn stars (Dworetzky 1993). Phosphorus ($Z = 15$) is overabundant in both stars, but not more so than its even- Z neighbours. Manganese ($Z = 25$) is slightly overabundant in HD 65949, but 2.5 dex in excess in HR 7143. Overall, we may conclude that the lighter elements of HR 7143 show a greater fractionation from the solar pattern than those of HD 65949.

When we consider the heavier elements, both stars show a large scatter, nearly exclusively of positive deviations from solar. Gallium

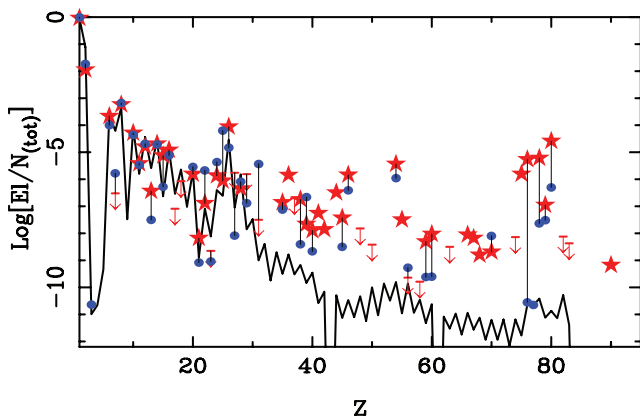


Figure 4. Solar abundances are again given by the solid black line. The stars or upper limit symbols again indicate abundances for HD 65949. Filled circles show abundances for HR 7143. When elements are determined in both stars, a vertical line connects the two values. Note the enormous difference in the osmium abundances ($Z = 76$).

is particularly notable, as it is some 3.7 dex overabundant in HR 7143. The upper limit in HD 65949 is about 1.7 dex. There is no indication of the stronger Ga II lines on the HARPS spectra. Apart from Ga and Y, the excesses in HR 7143 are lower than that in HD 65949. Note especially the case for Os ($Z = 76$) which is 5.3 dex in excess in HD 65949 but essentially solar in HR 7143.

Generally, among the elements heavier than zinc, the abundances in HD 65949 are more highly fractionated than those of HR 7143.

9.2 χ Lup

Abundances for χ Lup A [$T_{\text{eff}} = 10\,165$ K, $\log(g) = 3.8$, B9.5p HgMn] are given by Leckrone et al. (1999) as supplemented by papers cited by Wahlgren (2005). A plot of abundances versus Z reveals a relatively small scatter for most elements lighter than those with Z in the low 30's. This has been noted for HD 65949 and HR 7143. There are, however, several points for elements studied in the *HST* UV spectra. In particular, the marked *underabundance* of zinc ($Z = 30$) is prominent. The triplet Zn, Ga ($Z = 31$) and Ge ($Z = 32$) form an *even-Z* anomaly, incomprehensible from the point of view of nucleosynthesis. The same even- Z anomaly is shown by Ga, Ge and As. No marked overabundances occur in χ Lup until $Z = 33$. Beyond that value of Z , overabundances are common, and there are no underabundances for detected elements. Dworetzky, Persaud & Patel (2008) give $\log(\text{Xe}/\text{H}) = -5.74$, between the values for HR 7143 and HD 65949. There is no abundance for the noble gases Kr ($Z = 36$). Strontium ($Z = 38$) is enhanced in both HD 65949 and χ Lup. Barium ($Z = 56$) is significantly enhanced only in χ Lup and in HgMn stars, but not in HD 65949. Rhenium ($Z = 75$), so highly enhanced in HD 65949, has no detection in χ Lup. The overall very heavy element (Os, Pt, Au, Hg, Tl) enhancement in Chi Lup is present, but differs in detail from that of both HD 65949 and HR 7143.

We leave further discussion and possible interpretation of the χ Lup abundances to a future study.

10 DISCUSSION

10.1 The temperature differential

We reject the temperature differential, some 1100 K, as *primarily* responsible for the abundance differences discussed in the previous section. That is because similar abundance patterns persist in HgMn stars over comparable temperature ranges. Moreover, strong Hg and especially Pt are more common among cooler HgMn stars than hotter ones, and these elements are more abundant in the hotter star HD 65949 than the cooler star HR 7143. A similar argument applies to the Mn abundance, but with a reversed sense. Here the hotter HgMn stars are generally richer in Mn, but the cooler HR 7143 has the larger Mn abundance excess.

The isotopic composition of Hg in HD 65949 is also more typical of cooler HgMn stars than that of HR 7143. At low resolution, a mean wavelength of the Hg II feature may indicate an enrichment of the heavier isotopes – generally the cooler HgMn stars have longer centre-of-gravity wavelengths for the $\lambda 3984$ feature. However, for HR 7143, we measured a mean position of 3983.858 \AA , on a 2.4 \AA mm^{-1} plate taken at the Dominion Astrophysical Observatory (9682/10858u). This might be compared with the FEROS wavelength (cf. Paper I) of 3984.01 \AA for HD 65949. Synthesis of the higher resolution HARPS and UVES spectra available today prove that HD 65949 is richer in heavier Hg isotopes, though ^{204}Hg does not dominate, as in χ Lup.

10.2 Nuclear patterns

The elements Sr and Ba are typically associated with the s process. While the Sr excess is more than 2 dex, Ba is at most marginally enhanced, and could be depleted. This excludes the relevance of that process. On the other hand, the Solar system r process shows excesses at Te and Xe, and again, at Os and Pt. The former peak is associated with the $N = 82$ neutron shell closing, and the latter closed shell at $N = 126$. We have not reported an abundance for Te, but the element is positively identified, and surely in excess. Oscillator strength calculations currently under way will provide a quantitative result.

We have noted that the idea of mass transfer in connection with CP star anomalies is relatively old. Wahlgren et al. (1995) discuss it briefly in connection with the isotopic anomalies in χ Lup that suggest the r process. We note also, the shrewd observation of Woolf & Lambert (1999) that the stable, lighter Hg isotopes are never enhanced in HgMn stars, and that these are the only two isotopes *not* produced by the r process. On the other hand, Proffitt & Michaud (1989) concluded the likely transference of a significant amount of material from a nearby supernova to a B or A star was ‘one in a few thousand’. Even if HD 65949 represents that rare star, the abundances of the heavy elements are severely fractionated from a pure nuclear pattern. The anomalies *cannot* result only from an admixture of nuclear-processed material.

We therefore look within this pattern for some clue to the relevant fractionation mechanism. The favoured mechanism would be *in situ* separation by radiative and gravitationally driven diffusion.

10.3 Theoretical predictions

Surprisingly little theoretical work is of relevance to the present task. An exception is the decades-old but extensive work by Michaud et al. (1976, hereafter MCVV). In this work both time-scales, and extensive predictions are made through the lanthanide elements. In fig. 6 of MCVV there are precipitous abundance drops near $Z = 38$ –40 and 56–58. This suggests a depletion at Sr, which we do not see, and one at Ba, which we may. On the other hand, the calculations for the heavier elements were sufficiently rough that most elements were predicted to be overabundant by about the same amount. Only when relevant ions achieved the noble gas configurations (e.g. Sr III or Ba III) was there a significant reduction of the radiative to gravitational (plus temperature gradient) forces (g_R/g_{GT}). That ratio was more or less constant for most of the elements beyond $Z = 30$, and could not account for the structure seen in our Fig. 3.

The basic diffusion hypothesis has always been that the stars arrive on the main sequence with abundances that are well mixed. Chemical separation then took place as a result of a time-dependent process. Nevertheless, there has been almost no attempt to interpret abundances in terms of age.

The concept of age, as we need it here, need not be a chronological age, or years on the main sequence. MCVV and many subsequent studies (cf. Richer, Michaud & Turcotte 2000) added a ‘turbulent’ component to the diffusion coefficient. Without this modification much larger anomalies than those observed in some CP stars would be predicted. The more effective this turbulence, the slower the diffusion processes would be. Thus we must think of age in a relative sense. Chemical or cosmochemical maturity might be a more appropriate phrase than age.

For stars with masses above 2–2.6 M_\odot , MCVV found characteristic diffusion times very short with respect to the stellar lifetimes. They proceeded to predict abundance anomalies for these stars,

without consideration of the ages or the length of time since the diffusion began to operate. Presumably, this was because the time-scales were found to be very short, after which time an approximate equilibrium abundance pattern might be established.

This basic picture does not account for the occurrence of very different abundances in stars with similar temperatures and surface gravities.

10.4 Correlations

Suppose exotic material from a supernova were transferred to the surface of a nearby star. We must imagine the material to have characteristic r-process enhancements, and minor amounts of elements with $Z < 30$.

This material could be subject to grain condensation, followed by gas–grain separation as in the scenario proposed by Venn & Lambert (1990) to explain λ Boo stars. In our case, the elements that resist grain formation (Xe, Kr, Os, Pt, Hg) would be carried to the star. One might then expect to see a correlation of the abundance excesses with condensation temperatures (e.g. Lodders, 2003). However, we find no significant correlation of this kind.

We therefore favour a second model.

Fig. 5 shows that there is a correlation of the abundance excesses of the heavier elements with the second ionization potential. The significance of the correlation is 0.0013. The figure and significance calculation includes two points for Ba and Ce for which we have only upper limits. Should we exclude them, the significance drops to 0.016. However, if we use abundances for these elements decreased by 1 and even 2 dex, the significance of the correlation is essentially the same as with the upper limit, i.e. 0.0016.

While it is clear that factors other than the second ionization potential determine the overabundances, the correlation we find is unlikely to have arisen by chance.

The proposed model supposes that exotic r-processed material fell on to the star, and *then* was subject to *in situ* differentiation. One advantage of this model is that it would not require the diffusion of rhenium or mercury from great depths requiring the elements to pass through many ionization stages.

The ‘mass above the photosphere’ may be defined as $\int \rho dx$ from $x = 0$ to a physical depth where the optical depth is about unity. For late B stars, that mass is about 0.1 g cm^{-3} . This means that to enhance the Hg abundance by a factor of 2×10^6 , ions

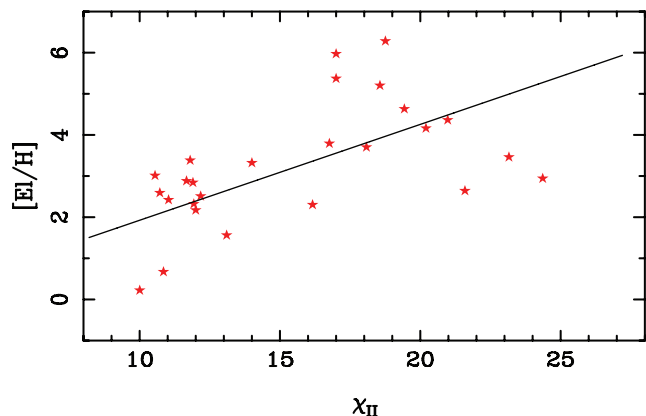


Figure 5. Logarithmic abundance excesses for elements with $Z > 30$ versus second ionization energies. Upper limits are not included. The line is a least-squares fit. The correlation coefficient 0.608 is significant at the 0.0013 level for 25 points.

would have to diffuse upward from a depth such that $\int \rho dx \approx 2 \times 10^5$. We use the $2.5 M_{\odot}$ model of P. Demarque, D. Guenther and J. Howard [cf. Cowley 1995, table 9.3(b)]. Numerical integration of the tabulated values show that at this depth ($r/R = 0.92$), $T = 4 \times 10^5$ K. If we use the Saha equation, taking the ratio of the relevant partition functions to be unity, we find the ratio of Hg^{+16} to Hg^{+15} approximately unity at this depth (9.6×10^4 km below the surface of the star).

This calculation assumed mercury that has diffused upward does not escape from the photosphere. We also have neglected lowering of the ionization energy. Both effects would increase the relevant degree of ionization. The ionization energy for $\text{Hg} \text{XVI}$ (+15) used here is from Carlson et al. (1970). The value 357 eV is approximate, but adequate for the present purposes, which is only to show the multiplicity of ion stages involved. The overall situation is not substantially different from that discussed by Cowley & Day (1976), where it was concluded that for an enhancement of 10^5 mercury would have to diffuse from depths involving $\text{Hg} \text{XI-XIII}$, and the relevant temperature (see Table 1, Model B) was 2×10^5 .

Diffusion from deep layers does not provide a basis for understanding the correlation with the second ionization potential.

10.5 Predictions

Based on the model of the preceding section, and the abundances of HD 65949 and HR 7143 (as typical of HgMn stars), we can make a number of predictions that can be checked by further investigation. The overall hypothesis is that both stars have been subject to exotic mass addition, but that HD 7143 is cosmochemically more mature than HD 65949.

(i) Osmium and rhenium are rarely (if ever) enhanced to the point where they are identified in ground-based spectra of HgMn stars. Therefore, these elements cannot be (strongly) supported by radiation in the atmospheres of HgMn stars compared, for example, to mercury. (Their high abundance in HR 65949 must result from a very recent transfer of material.)

(ii) Xenon is often found in HgMn stars. In spite of the fact that Xe I has noble gas structure, significant support for this element must exist. The case of Kr needs more observational material. Though it is not seen in HgMn stars, better observations could lead to its identification. We see no indication of $\text{Kr II } \lambda 4355.48$ in HR 7143 on CH04 material posted on Castelli's web site.

(iii) The nitrogen deficiency and the phosphorus excess must be established rapidly in HD 65949. These anomalies appear before a significant Mn excess appears.

(iv) The large gallium abundance shown by many HgMn stars is not seen in HD 65949. Therefore, it must be pushed up from considerable depths, on a time-scale longer than relevant for HD 65949. It would be a pure diffusion anomaly.

Of course, it may be possible to account for the abundance pattern of HR 65949 with the fundamental diffusion picture when the necessary atomic data are known. The lack of barium enhancement may already be explained in MCVV. The overall scatter of the heavier elements could be attributed to the relative ease of transport of atoms with initially low abundances. This would mean that mercury and rhenium were pushed up from deep layers where atoms might be 10-fold or more fold ionized. We would then conclude that the observed correlation with second ionization potential was a red herring.

ACKNOWLEDGMENTS

We thank P. North and B. Smalley for computer codes, and J. R. Fuhr, J. Reader and W. Wiese of NIST for advice on atomic data and processes. Thanks also to J. J. Cowan for comments on the abundance pattern in HD 65949 from the point of view of nucleosynthesis. This research has made use of the SIMBAD data base, operated at CDS, Strasbourg, France. Our calculations have made extensive use of the VALD atomic data base (Kupka et al. 1999). Thanks are also due to M. Netopil for help during observations in 2008 August. CRC thanks John Hutchings, Murray Fletcher and his colleagues at Michigan, especially Ming Zhao, for numerous ideas and comments. Thanks are due to J. Andersen and G. Torres for a preprint of their review paper on the masses and radii of normal stars. Financial support of the Belgian FRS-FNRS is also acknowledged. GMW acknowledges support from NASA grant NNG06GJ29G.

REFERENCES

- Abt H. A., Levy S. G., 1972, *ApJ*, 172, 355
 Abt H. A., Morgan W. W., 1969, *AJ*, 74, 813
 Adelman S. J., Snow T. P., Wood E. L., Ivans I. I., Sneden C., Ehrenfreund P., Foing B. H., 2001, *MNRAS*, 328, 1144
 Asplund M., Grevesse N., Sauval A. J., Scott P., 2009, *ARA&A*, 47, 481
 Biémont E., Grevesse N., Kwiatowski M., Zimmerman P., 1982, *A&A*, 108, 127
 Biémont E., Palmeri P., Quinet P., 1999, *Ap&SS*, 269–270, 635. See also the online data base: <http://w3.umh.ac.be/~astro/dream.shtml>
 Blaise J., Wyart J.-F., 2009, online data tables: <http://www.lac.u-psud.fr/Database/Contents.html>
 Carlson T. A., Nestor C. W., Jr, Wasserman N., McDowell J. D., 1970, *Atomic Data*, 2, 63
 Castelli F., 2009, www.user.oats.ts.astro.it/castelli/
 Castelli F., Hubrig S., 2004, *A&A*, 425, 263 (CH04)
 Cowan R. D., 1981, *The Theory of Atomic Structure and Spectra*. California Univ. Press, Berkeley, CA
 Cowley C. R., 1971, *Observatory*, 91, 139
 Cowley C. R., 1995, *An Introduction to Cosmochemistry*. Cambridge Univ. Press, Cambridge
 Cowley C. R., Barisciano L. P., Jr, 1994, *Observatory*, 114, 308
 Cowley C. R., Day C. A., 1976, *ApJ*, 205, 440
 Cowley C. R., Wahlgren G. M., 2006, *A&A*, 447, 681
 Cowley C. R., Hubrig S., González G. F., Nuñez N., 2006, *A&A*, 455, L21 (Paper I)
 Cowley C. R., Hubrig S., Wahlgren G. M., 2008, *J. Phys. Conf. Ser.*, 130, 12005 (Paper II)
 Dekker H., D'Odorico S., Kaufer A., Delabre B., Kotzlowski H., 2000, in Iye M., Moorwood A. F. M., eds, *Proc. SPIE Vol. 4008, Optical and IR Telescope Instrumentation and Detectors*. SPIE, Bellingham, p. 534
 Dolk L., Litzén U., Wahlgren G. M., 2002, *A&A*, 388, 692
 Dworetsky M. M., 1993, in Dworetsky M. M., Castelli F., Faraggiana R., eds, *ASP Conf. Ser. Vol. 44, Peculiar Versus Normal Phenomena in A-Type and Related Stars*. Astron. Soc. Pac., San Francisco, p. 1
 Dworetsky M. M., Storey P. J., Jacobs J. M., 1984, *Phys. Scr.*, T8, 39 (DSJ)
 Dworetsky M. M., Persaud J. L., Patel K., 2008, *MNRAS*, 385, 1523
 Engleman R., 1989, *ApJ*, 340, 1140
 Fivet V., Quinet P., Biémont É., Xu H. L., 2007, *J. Electron Spectrosc. Related Phenomena*, 156–158, 250
 Fivet V. et al., 2009, *MNRAS*, 396, 2124
 Fuhr J. R., Wiese W. L., 1996, in Lide D. R., ed., *CRC Handbook of Chemistry & Physics, NIST Atomic Transition Probability Tables*, 77th edn. CRC Press, Boca Raton, FL
 Fuhr J. R., Wiese W., 2006, *J. Phys. Chem. Reference Data*, 35, 1669
 Giesekeing F., 1978, *A&AS*, 32, 17
 Giesekeing F., Karimie M. T., 1982, *A&AS*, 49, 497
 González J. F., Lapasset E., 2000, *AJ*, 119, 2296
 Guthrie B. N. G., 1971, *Ap&SS*, 10, 156

- Hauck B., Mermilliod M., 1998, *A&AS*, 129, 431
- Hubrig S., North P., Schöller M., Mathys G., 2006, *Astron. Nachr.*, 327, 289
- Ivarsson S., Wahlgren G. M., Dai Z., Lundberg H., Leckrone D. S., 2004, *A&A*, 425, 353
- Kaufer A., Stahl O., Tubbesing S., Nørregaard P., Avila G., Francois P., Pasquini L., Pizzella A., 1999, *ESO Messenger*, 95, 8
- Klinkenberg P. F. A., Meggers W. F., Velasco R., Catalan M. A., 1957, *J. Res. Natl. Bureau Standards*, 59, 319
- Kramida A. E., Shirai T., 2006, *J. Phys. Chem. Reference Data*, 35, 423
- Kunzli M., North P., Kurucz R. L., Nicolet B., 1997, *A&AS*, 122, 51
- Kupka F., Piskunov N. E., Ryabchikova T. A., Stempels H. C., Weiss W. W., 1999, *A&AS*, 138, 119
- Kurucz R. L., 1993, *Smithsonian Astrophys. Obser.*, CD-ROM No. 18
- Kurucz R. L., 1995, *Smithsonian Astrophys. Obser.*, CD-ROM No. 23
- Leckrone D. S., Proffitt C. R., Wahlgren G. M., Johansson S. G., Brage T., 1999, *AJ*, 117, 1454
- Ljung G., Nilsson H., Asplund M., Johansson S., 2006, *A&A*, 456, 1181
- Lodders K., 2003, *ApJ*, 591, 1220
- Mayor M., Pepe F., Queloz D. et al., 2003, *ESO Messenger*, 114, 20
- Meggers W. F., Catalan M. A., Sales M., 1958, *J. Res. Natl. Bureau Standards*, 61, 441
- Meggers W. F., Corliss C. H., Scribner B. F., 1975, *NBS Monograph*, 145
- Meléndez J., Barbuy B., 2009, *A&A*, 497, 611
- Mermilliod J.-C., Hauck B., Mermilliod M., 2007, *General Catalogue of Photometric Data*, <http://www.unige.ch/sciences/astro/>
- Michaud G., 1970, *ApJ*, 160, 641
- Michaud G., Charland Y., Vauclair S., Vauclair G., 1976, *ApJ*, 210, 447 (MCVV)
- Moon T. T., 1984, *Communications Univ. London Obser.*, 78
- Moon T. T., Dworetzky M. M., 1985, *MNRAS*, 217, 305
- Moore C. E., 1949–1958, *Atomic Energy Levels, Vols I–III*, NBS Circ., 467. US Government Printing Office, Washington, DC
- Munari U., Zwitter T., 1997, *A&A*, 318, 269
- Nilsson H., Ivarsson S., 2008, *A&A*, 492, 609
- Nilsson H., Ljung G., Lundberg H., Nielsen K. E., 2006, *A&A*, 445, 1165
- Palmeri P., Quinet P., Biémont É., Xu H. L., Svanberg S., 2005, *MNRAS*, 362, 1348
- Palmeri P., Quinet P., Biémont É., Svanberg S., Xu H. L., 2006, *Phys. Scr.*, 74, 297
- Palmeri P. et al., 2009, *J. Phys. B*, 42, 165005
- Paunzen E., Schnell A., Maitzen H. M., 2006, *A&A*, 458, 293
- Pickering J. C., Thorne A. P., Perez R., 2001, *ApJS*, 132, 403 (Erratum: *ApJS*, 138, 247, 2002)
- Pintado O. I., Adelman S. J., 2003, *A&A*, 406, 987
- Preston G. W., 1974, *ARA&A*, 12, 257
- Proffitt C. R., Michaud G., 1989, *ApJ*, 345, 998
- Quinet P., 2002, *J. Phys. B*, 35, 19
- Quinet P., Palmeri P., Biémont É., Jorissen A., Van Eck S., Svanberg S., Xu H. L., Plez B., 2006, *A&A*, 448, 1207
- Quinet P., Palmeri P., Fivet V., Biémont É., Nilsson H., Engström L., Lundberg H., 2008, *Phys. Rev. A*, 77, 022501 (QPFb)
- Ralchenko Yu., Kramida A. E., Reader J., NIST ASD Team, 2008, *NIST Atomic Spectra Database (version 3.1.5)* (online). National Institute of Standards and Technology, Gaithersburg, MD [available at <http://physics.nist.gov/asd3> (launched on 2010 January 24)]
- Reader J., Corliss C. H., 1980, *NSRDS-NBS Monograph*, 68
- Richer J., Michaud G., Turcotte S., 2000, *ApJ*, 529, 338
- Rosberg M., Wyart J.-F., 1997, *Phys. Scr.*, 55, 690
- Ryabchikova T., Piskunov N., Savanov I., Kupka F., Malanushenko V., 1999, *A&A*, 343, 229
- Ryabchikova T., Ryabtsev A., Kochukhov O., Bagnulo S., 2006, *A&A*, 456, 329
- Sansonetti C. J., Andrew K. L., 1986, *JOSA*, B3, 386
- Sansonetti C. J., Reader J., 2001, *Phys. Scr.*, 63, 219
- Smirnov Yu. M., Shapochkin M. B., 1979, *Opt. Spectrosc.*, 47, 243
- Torres G., Andersen J., Giménez A., 2010, *A&AR*, 18, 67
- Unsöld, A., 1955, *Physik der Sternatmosphären, Zweite Aufl.* Springer-Verlag, Berlin
- van Leeuwen F., 2009, *A&A*, 497, 209
- Venn K. A., Lambert D. L., 1990, *ApJ*, 363, 234
- Wahlgren G. M., 2005, in Zverko J., Žižňovský J., Adelman S. J., Weiss W. W., eds, *The A-Star Puzzle*. Cambridge Univ. Press, Cambridge, p. 291
- Wahlgren G. M., Leckrone D. S., Johansson S. G., Rosberg M., Brage T., 1995, *ApJ*, 444, 438
- Wahlgren G. M., Johansson S., Litzén, U., Gibson N. D., Cooper J. C., Lawler J. E., Leckrone D., Engleman R., Jr, 1997, *ApJ*, 475, 380
- Wolk S. J., Harnden F. R., Jr, Murray S. S. et al., 2004, *ApJ*, 606, 466
- Woolf V., Lambert D. L., 1999, *ApJ*, 521, 414
- Wyart J.-F., 1977, *Opt. Pura Aplicada*, 10, 177
- Wyart J.-F., Tchang-Brillet W.-U. L., Churilov S. S., Ryabtsev A. N., 2008, *A&A*, 483, 339
- Zielińska S., Bratasz Ł., Dzierżęga K., 2002, *Phys. Scr.*, 66, 454

APPENDIX A: DISCUSSION OF INDIVIDUAL ABUNDANCES

The MICHIGAN software used to obtain abundances from individual lines is set up to read a data base that is basically VALD, but with numerous additions and edits. For example, for the third spectra of the lanthanides, all values are from the DREAM site. Use of data from original sources often requires line-by-line editing. To avoid this in many cases, we used our default data base, but checked against more recent sources, or against the posting on the NIST site, and if the differences were minor, we did not recompute an abundance.

All averages are logarithmic, that is, the logarithms of abundances for individual lines were averaged directly.

Original sources of oscillator strengths are cited where practicable, but we relied heavily on the online data bases of Ralchenko et al. (2008, NIST), Kupka et al. (1999, VALD) and Biémont et al. (1999, DREAM). When no source of oscillator strength is explicitly cited, the values come from VALD.

In the following sections, a measured stellar wavelength is indicated by an asterisk, e.g. $\lambda^*4911.66$.

Helium [$Z = 2$; $\log(\text{He}/N_{\text{tot}}) \approx -1.95 \pm 0.14$]: a rough estimate, using Voigt profiles of 8 He I lines. The helium abundance is about 10 per cent that of the sun.

Carbon [$Z = 6$; $\log(\text{C}/N_{\text{tot}}) = -3.66 \pm 0.4$]: the abundance is from a synthesis of the C II $\lambda 4267$ doublet, which is clearly present. The VALD oscillator strengths are very close to those on the NIST site. A few C I and C II lines are surely present, but give inconsistent abundances, most likely due to blends. The carbon abundance is nearly solar. CH04 find a ca. 0.5 dex deficiency of carbon.

Nitrogen [$Z = 7$; $\log(\text{N}/N_{\text{tot}}) \leq -6.52$]: neither N I nor N II can be positively identified. An upper limit of 0.3 mÅ for N II $\lambda 8680$ gives $\log(\text{N}/N_{\text{tot}}) = -6.52$, corresponding to a deficiency of about 2.4 dex with respect to the sun. CH04 got an upper limit corresponding to a deficiency of -1.7 dex in HR 7143.

Oxygen [$Z = 8$; $\log(\text{O}/N_{\text{tot}}) = -3.24 \pm 0.16$]: nine O I lines, excluding the strong triplet $\lambda\lambda 7772, 7774$ and 7775 yield a small oxygen excess above to the solar value. Oscillator strengths are from VALD but agree well with NIST. CH04 also find a slight excess of oxygen for HR 7143.

Neon [$Z = 10$; $\log(\text{Ne}/N_{\text{tot}}) = -4.29 \pm 0.16$]: a close examination of the HARPS spectra show that Ne I is clearly present. The abundance is based on 10 weak lines and oscillator strengths from NIST. The line-to-line agreement is excellent.

Sodium [$Z = 11$; $\log(\text{Na}/N_{\text{tot}}) = -5.42 \pm 0.13$]: the abundance is from the D-lines, with equivalent widths of 27 and 21 mÅ. The

probable error is the difference of the two determinations. The stellar lines are much weaker than the interstellar ones.

Magnesium [$Z = 12$; $\log(\text{Mg}/N_{\text{tot}}) = -4.80 \pm 0.45$]: the adopted abundance is primarily from nine Mg II lines, which give -4.91 ± 0.17 . We did not use the $\lambda 4481$ doublet for an abundance. Four Mg I lines, including the b-lines give -4.46 ± 0.47 , which might indicate stratification or too hot a model. They are weighted 1/3 in the adopted value. The adopted error is the difference in the Mg I and Mg II values. Oscillator strengths are from VALD, but are very close to those at the NIST site.

Aluminium [$Z = 13$; $\log(\text{Al}/N_{\text{tot}}) = -6.45 \pm 0.24$]: the two strongest Al II lines, $\lambda\lambda 4663.05$ and 6243.36 were measured and so identified in the online wavelength list: <http://www.astro.lsa.umich.edu/~cowley/hd65949/>. A 5.8-mÅ line is present at the position of the strong Al I line $\lambda 3691.52$. This is almost certainly the line 3691.49 on the online list. There is no definite feature at the position of the other strong Al I line, $\lambda 3944.01$. However, the noise might obscure a 1-mÅ feature. We adopt a straight average of two Al I and two Al II lines. Oscillator strengths were from VALD, but are very close to NIST. Aluminium is deficient. This result was also found by CH05.

Silicon [$Z = 14$; $\log(\text{Si}/N_{\text{tot}}) = -4.69 \pm 0.26$]: the abundance is from 10 Si II and two Si III lines with equivalent widths ranging from 4.6 to 136 mÅ. Oscillator strengths are mostly from NLTE LINES (Kurucz 1993). Generally, the agreement with NIST was good. However, for $\lambda\lambda 5669$ and 5957 , we substituted the NIST values, which had B+ accuracy.

The 2 Si III lines, $\lambda\lambda 4552$ and 4567 yield abundances of -4.29 and -4.46 , in fair agreement with the overall mean. Both lines have NIST graded B+ accuracies.

Phosphorus [$Z = 15$; $\log(\text{P}/N_{\text{tot}}) = -5.13 \pm 0.29$]: the abundance is based on 19 weak P II lines. Oscillator strengths are from BELLIGHT (Kurucz 1993), a compilation from various sources. The overabundance, some 1.6 dex, is substantially above that found by CH04 for HR 7143.

Sulphur [$Z = 16$; $\log(\text{S}/N_{\text{tot}}) = -4.92 \pm 0.24$]: the abundance is based on 34 S II lines with equivalent widths from 1.3 to 17 mÅ. Two outliers, $\lambda\lambda 4162$ and 4174 were excluded from the average. The abundance is solar, within the uncertainties. CH04 find sulphur underabundant by 0.4 dex in HR 7143.

Chlorine [$Z = 17$; $\log(\text{Cl}/N_{\text{tot}}) \leq -7.09$]: an upper limit is derived from Cl II $\lambda 4794.55$, which is ≤ 0.3 mÅ. The oscillator strength is from Fuhr & Wiese (1996).

Argon [$Z = 18$; $\log(\text{Ar}/N_{\text{tot}}) \leq -6.07$]: an upper limit is derived from the strong Ar I line $\lambda 8115.31$. The oscillator strength is from Fuhr & Wiese (1996).

Calcium [$Z = 20$; $\log(\text{Ca}/N_{\text{tot}}) = -5.81 \pm 0.53$]: the strongest Ca I line, $\lambda 4227$ is probably present. We measured a 1.6-mÅ line just above the noise level. There were seven unblended Ca II lines. With a microturbulence, $\xi_t = 1 \text{ km s}^{-1}$, the K-line and $\lambda\lambda 8498$ and 8542 of the infrared triplet yield an abundance ca. 1 dex higher than the weaker lines, $\lambda\lambda 3706$, 8201 , 8248 and 8912 . The plot of abundance versus equivalent width looks like a classic case of too low a microturbulence. The adopted mean is the average of assuming $\xi_t = 1$ and $\xi_t = 5 \text{ km s}^{-1}$. The latter brings strong and weak Ca II lines into agreement. The uncertainty is the difference in these abundances. We do not consider $\xi_t = 5 \text{ km s}^{-1}$ realistic. Interestingly, the strong Ca II lines agree with the very weak Ca I $\lambda 4227$ line. Calcium is poorly determined; the source of the large uncertainty is not understood. The usual culprits are non-local thermodynamic equilibrium (NLTE) or stratification. They are not explored here. Note that the Ca II K-line and the two components

of the infrared triplet are the strongest lines used in the present analysis.

Scandium [$Z = 21$; $\log(\text{Sc}/N_{\text{tot}}) = -8.18 \pm 0.07$]: the abundance is based on five Sc II lines, including $\lambda 4246$ with equivalent widths from 5.1 to 16.8 mÅ. The internal agreement is good; the standard deviation for the five lines is less than 0.1 dex.

Titanium [$Z = 22$; $\log(\text{Ti}/N_{\text{tot}}) = -6.90 \pm 0.27$]: only Ti II lines are available. The abundance is based on 42 lines with equivalent widths ranging from 2 to 45 mÅ. Oscillator strengths are from Pickering, Thorne & Perez (2001). Results were very similar if lines with LS-allowed transitions from Kurucz (1995, used by VALD) were used. No significant trends of abundances with wavelength, equivalent width or excitation potential were noted. Three obvious outliers were excluded. If they are averaged in, the abundance would be -6.78 .

Vanadium [$Z = 23$; $\log(\text{V}/N_{\text{tot}}) \leq -8.65$]: while V II lines are prominent in the spectra of cooler Am and superficially normal A stars; the lines are typically weak or absent in hotter CP types. We estimate an upper limit taking the equivalent width of V II $\lambda 3545.19$ to be ≤ 0.5 mÅ. This is close to the upper limit found for vanadium by CH04.

Chromium [$Z = 24$; $\log(\text{Cr}/N_{\text{tot}}) = -5.87 \pm 0.31$]: there is an ≈ 1 -mÅ feature at the proper position to be $\lambda 4254.35$, the strongest Cr I line in the region. That line alone gives an abundance of $\log(\text{Cr}/N_{\text{tot}}) = -5.6$ in satisfactory agreement with the overall mean of the Cr II lines. The abundance is based on 64 LS-permitted transitions. Only 14 of the 64 lines used were found in the online material published by Nilsson et al. (2006). A comparison of the LS-permitted lines in VALD and Nilsson et al. (2006) gave a mean of $+0.045$ for $\log(gf_{\text{VALD}}) - \log(gf_{\text{Nilsson}})$, with a standard deviation of 0.16 dex. This difference was considered negligible at the present level of accuracy. There is a slight trend of abundance with equivalent width that can be removed by assuming $\xi_t = 3 \text{ km s}^{-1}$. The resulting average abundance would be -5.98 ± 0.26 . Since Cr has an even Z , and hyperfine broadening is not anticipated, we retained the result with $\xi_t = 1$ for consistency with other spectra.

Manganese [$Z = 22$; $\log(\text{Mn}/N_{\text{tot}}) = -6.06 \pm 0.15$]: there is no indication of Mn I. The abundance is based on 22 Mn II lines with strengths ranging from 3.1 to 86 mÅ. There was no trend of abundance with equivalent width with $\xi_t = 2.0 \text{ km s}^{-1}$. Abundances using 1.0 and 3.0 km s^{-1} showed slight trends. Only LS-allowed transitions were used. We eliminated three outliers after noting their transitions were not LS-allowed, but which had not been caught by our filter.

Iron [$Z = 26$; $\log(\text{Fe}/N_{\text{tot}}) = -4.06 \pm 0.24$]: the adopted abundance is from 98 Fe II lines. Seven Fe III lines give -4.09 , while 21 Fe I lines give -3.72 ± 0.37 . In view of possible stratification we do not consider these values. However, with the cooler model used in Paper II, we obtained -3.96 , in better agreement with Fe II and Fe III, as detailed in Paper II. Oscillator strengths for the first two spectra were from Fuhr & Wiese (1996). For Fe II, the recent values of Meléndez & Barbuy (2009) made only a 0.01 dex in the average abundance from Fe II using transitions from Fuhr & Wiese (2006). The iron abundance is about a factor of 3 above the solar value.

Cobalt [$Z = 27$; $\log(\text{Co}/N_{\text{tot}}) \leq -5.76$]: neither Co I nor Co II is firmly identified. An approximate upper limit is set by the absence of the strong Co I line $\lambda 3443.64$. If the equivalent width were 0.5 mÅ, the abundance of Co would be -5.76 . The strong Co II line $\lambda 4062.73$ gives an upper limit -5.33 , assuming 0.8 mÅ .

Nickel [$Z = 28$; $\log(\text{Ni}/N_{\text{tot}}) = -6.35 \pm 0.31$]: the presence of Ni I cannot be confirmed. While a definite line (7 mÅ) is present within 0.01 \AA of the resonance line in multiplet 19, the *next* strongest

line in that multiplet is absent, as are the next strongest four Ni I lines in Meggers, Corliss & Scribner (1975). Ni II is surely present, although weak. The abundance is based on 5 lines with measured equivalent widths from 4.3 to 10 mÅ.

Copper [$Z = 29$; $\log(\text{Cu}/N_{\text{tot}}) \leq -5.81$]: an upper limit was set from Cu I $\lambda 5153.24$, and equivalent width possibly 2 mÅ. An examination of the region of the strongest expected lines did not confirm the identification.

Zinc [$Z = 30$; $\log(\text{Zn}/N_{\text{tot}}) \leq -7.8$]: we can only set an upper limit that is roughly solar. An ≈ 5 mÅ line measured at $\lambda^*4911.66$ near the position of Zn II $\lambda 4911.63$ may be entirely due to a Nd III line tabulated by Ryabchikova et al. (2006). If any Zn II feature is present, it is at the level of the noise.

Ga through Selenium ($Z = 31$ – 34): Neither the first nor the second spectrum of any of these elements can be confirmed to be present. We report an upper limit for gallium of -7.50 , based on an equivalent width of $\lambda 4251.14$ of 0.4 mÅ.

Bromine [$Z = 35$; $\log(\text{Br}/N_{\text{tot}}) = -6.81 \pm 0.5$]: The wavelength agreement was very good on two HARPS spectra for the three lines with oscillator strengths on the NIST web site. Equivalent widths for Br II $\lambda\lambda 4704.9, 4785.5$ and 4816.7 of 4.1, 2.4 and 0.4 mÅ yield $\log(\text{Br}/N_{\text{tot}})$ of $-6.64, -6.69$ and -7.39 . We use weight 1/2 for the weakest line. The error is an estimate. Br II is rarely observed in late B stars, but two of these lines were used by CH04, and all three were observed in three Cen A (Cowley & Wahlgren 2006). Br II is judged weakly present in HD 65949.

Krypton [$Z = 36$; $\log(\text{Kr}/N_{\text{tot}}) = -5.85 \pm 0.13$]: five weak Kr II lines on HARPS spectra have good wavelength agreement with their laboratory values; the derived abundances are all within a factor of 2 of one another. The spectrum is weak, but present beyond doubt. There are no Kr II lines in the VALD or Kurucz data bases. We used transition probabilities from the NIST site.

Rubidium [$Z = 37$; $\log(\text{Rb}/N_{\text{tot}}) \leq -6.70$]: a search for the strongest NIST lines in the region observed did yield some possible features for Rb II. The upper limit is based on an equivalent width of 1.2 mÅ for Rb II $\lambda 4244.40$, measured at 4244.41 on a HARPS spectrum. The oscillator strength is from Smirnov & Shapochkin (1979).

Strontium [$Z = 38$; $\log(\text{Sr}/N_{\text{tot}}) = -6.76 \pm 0.45$]: the Sr II resonance lines are unmistakable, and give abundances ranging from -6.6 to -6.2 , depending on the method of analysis (synthesis versus equivalent width). We consider these lines to be affected by NLTE or stratification. The abundance is quite uncertain. We take it from the subordinate lines, $\lambda\lambda 4161$ and 4305 . Two very weak lines $\lambda\lambda 4312.77$ and 4414.84 yield significantly higher abundances. We reject them as probably due to severe blending. The oscillator strengths are from VALD, but are not significantly different from NIST.

Yttrium [$Z = 39$; $\log(\text{Y}/N_{\text{tot}}) = -7.66 \pm 0.11$]: the abundance is based on 14 Y II lines from 3327 to 5662 Å with equivalent widths from 1.3 to 18.4 mÅ. Oscillator strengths are from VALD. Lines in common agree with Fuhr & Wiese (1996).

Zirconium [$Z = 40$; $\log(\text{Zr}/N_{\text{tot}}) = -7.90 \pm 0.17$]: our rough estimate is based on three Zr II lines with equivalent widths of 5.0, 9.4 and 9.6 mÅ. Oscillator strengths from VALD but for these lines agree sufficiently with Ljung et al. (2006)

Niobium [$Z = 41$; $\log(\text{Nb}/N_{\text{tot}}) = -7.26 \pm 0.29$]: the abundance is based on 22 lines with equivalent widths from 1.6 to 20 mÅ. The transition probabilities were mostly taken from Nilsson & Ivarsson (2008). Values for $\lambda\lambda 3517$ and 4119 are from VALD. Nb II is not routinely identified in CP stars; CH04 do not report an abundance for niobium in HR 7143. Niobium creates

an odd- Z anomaly, being more abundant than its adjacent even- Z neighbours.

Molybdenum [$Z = 42$; $\log(\text{Mo}/N_{\text{tot}}) = -7.86 \pm 0.34$]: the entry in Table 3 is based on four quite weak Mo II lines, with one outlier weighted 1/2. Oscillator strengths are from Quinet (2002).

Ruthenium [$Z = 44$; $\log(\text{Ru}/N_{\text{tot}}) = 6.50 \pm 0.48$]: the abundance is based on 20 Ru II lines with equivalent widths ranging from 0.3 to 22 mÅ. We used new oscillator strengths and partition functions recently calculated by the Mons group (Palmeri et al. 2009).

Rhodium [$Z = 45$; $\log(\text{Rh}/N_{\text{tot}}) \approx -7.43$]: the abundance is based on only one strong Rh II line in multiplet 5, i.e. $\lambda 3307.37$. The (guessed) oscillator strength, $\log(gf) = 0.00$ is from Kurucz (1993). CH05 attributed seven features to Rh II. Five of these lines are below the UV cut-off of our spectra.

Palladium [$Z = 46$; $\log(\text{Pd}/N_{\text{tot}}) = -5.84 \pm 0.14$]: the result is based on four weak Pd II lines, and one blended feature. The abundances from the four lines are within a factor of 2 of one another. Oscillator strengths are from Biémont, Grevesse & Kwiatowski (1982).

Silver through tellurium ($Z = 47$ – 52):

(i) There is no support for either Ag I or Ag II from searches for the strongest lines within our wavelength coverage.

(ii) We find only marginal evidence for Cd. The upper limit is from Cd II $\lambda 4415.8$, possibly present as a 1-mÅ asymmetry to the violet of a stronger, unidentified line, probably Re II.

(iii) A search for the strongest lines yields no support for the presence Sb II.

(iv) We derive an upper limit of $\log(\text{Sn}/N_{\text{tot}}) \approx -8.42$ by assuming Sn II $\lambda 6453.5$ has an equivalent width of 1 mÅ. The oscillator strength used was from NIST.

(v) Tellurium: Te II is surely present. Oscillator strengths are currently being calculated, and will be reported in due course.

Xenon [$Z = 54$; $\log(\text{Xe}/N_{\text{tot}}) = -5.42 \pm 0.11$]: the abundance is based on six Xe II lines with equivalent widths from 5 to 27 mÅ. Transition probabilities are from Zielińska, Bratasz & Dzierżęga (2002). The wavelength agreement is excellent. The spectrum is securely identified.

Cesium [$Z = 55$; $\log(\text{Cs}/N_{\text{tot}}) \leq -7.7$]: a single, weak feature centred at $\lambda^*4603.78$ provides an upper limit to the Cs abundance. The stellar feature is not broad enough to fit the laboratory hfs (Sansonetti & Andrew 1986), though a partial contribution from Cs II cannot be excluded. The upper limit falls between the abundance of xenon, and an upper limit for barium.

Barium [$Z = 56$; $\log(\text{Ba}/N_{\text{tot}}) \leq -9.64$]: the Ba II resonance line $\lambda 4554$ has an equivalent width no larger than about 0.6 mÅ. There is no indication of the presence of the second component of the doublet, $\lambda 4934$.

Cerium [$Z = 58$; $\log(\text{Ce}/N_{\text{tot}}) \leq -9.79$]: the upper limit is based on the non-appearance of the strong Ce III line $\lambda 3454.39$, for which we estimate from raw UVES scans that the equivalent width cannot be larger than about 0.1 mÅ. Because of the wavelength placement and intensity distribution of Ce III, it is more rarely identified in CP stars. The oscillator strength used for $\lambda 3454$ was from the DREAM site.

Praseodymium [$Z = 59$; $\log(\text{Pr}/N_{\text{tot}}) = -8.31 \pm 0.21$]: the abundance is based on 16 Pr III lines from 4 to 20 mÅ. The oscillator strengths are from the DREAM site and line-to-line agreement is good (± 0.21 s.d.). The strongest likely Pr II lines are blended. An equivalent width of 0.5 mÅ for $\lambda 4225$ yields an upper limit of -7.9

Table B1. New partition functions for Ru, Re and Os atoms and ions.

T (K)	Ru I ^a	Ruthenium Ru II ^b	Ru III ^b	Re I ^c	Rhenium Re II ^d	Re III ^e	Os I ^f	Osmium Os II ^g	Os III ^h
3000	22.33	17.13	16.47	6.10	7.03	6.02	12.80	13.40	11.85
3500	24.92	18.65	17.40	6.27	7.08	6.05	14.28	14.79	12.87
4000	27.72	20.25	18.27	6.55	7.18	6.12	15.93	16.31	13.93
4500	30.75	21.94	19.13	6.98	7.36	6.24	17.75	17.97	15.02
5000	34.01	23.73	20.03	7.58	7.63	6.43	19.74	19.77	16.15
5500	37.49	25.62	20.98	8.38	8.01	6.69	21.92	21.70	17.33
6000	41.20	27.60	21.99	9.39	8.53	7.04	24.29	23.77	18.56
6500	45.15	29.68	23.09	10.62	9.18	7.48	26.87	25.98	19.85
7000	49.37	31.85	24.25	12.10	9.98	8.02	29.65	28.33	21.22
7500	53.87	34.10	25.49	13.83	10.95	8.67	32.67	30.83	22.66
8000	58.70	36.45	26.80	15.84	12.20	9.41	35.93	33.46	24.18
8500	63.90	38.87	28.17	18.15	13.41	10.26	39.45	36.24	25.78
9000	69.53	41.39	29.60	20.78	14.91	11.22	43.27	39.16	27.47
9500	75.64	43.98	31.08	23.76	16.58	12.27	47.41	42.21	29.23
10000	82.30	46.66	32.61	27.11	18.45	13.43	51.90	45.41	31.08
10500	89.58	49.42	34.18	30.88	20.50	14.68	56.79	48.73	33.01
11000	97.55	52.27	35.79	35.20	22.74	16.03	62.10	52.19	35.03
11500	106.29	55.21	37.43	39.79	25.16	17.48	67.89	55.79	37.12
12000	115.88	58.23	39.10	45.01	27.78	19.01	74.19	59.53	39.28
12500	126.39	61.35	40.81	50.80	30.58	20.64	81.07	63.40	41.53
13000	137.89	64.56	42.54	57.20	33.58	22.34	88.55	67.41	43.84
13500	150.45	67.87	44.29	64.25	36.77	24.14	96.69	71.56	46.23
14000	164.15	71.28	46.08	71.99	40.16	26.01	105.55	75.86	48.69
14500	179.06	74.81	47.88	80.48	43.75	27.96	115.16	80.31	51.21
15000	195.22	78.45	49.71	89.75	47.53	29.98	125.58	84.91	53.80
15500	212.70	82.22	51.56	99.85	51.52	32.08	136.84	89.67	56.46
16000	231.54	86.12	53.44	110.82	55.73	34.25	148.99	94.60	59.18
16500	251.81	90.16	55.34	122.69	60.14	36.49	162.08	99.71	61.96
17000	273.53	94.34	57.27	135.50	64.78	38.79	176.13	104.99	64.80
17500	296.75	98.69	59.22	149.30	69.63	41.16	191.18	110.46	67.71
18000	321.50	103.22	61.20	164.10	74.73	43.59	207.27	116.12	70.67
18500	347.80	107.92	63.20	179.95	80.05	46.20	224.41	121.98	73.70
19000	375.69	112.82	65.24	196.86	85.63	48.64	242.65	128.06	76.78
19500	405.17	117.94	67.30	214.87	91.46	51.25	261.99	134.35	79.92
20000	436.27	123.27	69.39	233.99	97.54	53.92	282.46	140.88	83.13
20500	469.00	128.85	71.52	254.24	103.90	56.64	304.07	147.64	86.39
21000	503.35	134.68	73.68	275.64	110.53	59.42	326.84	154.64	89.71
21500	539.34	140.78	75.87	298.20	117.44	62.25	350.76	161.91	93.20
22000	576.97	147.16	78.10	321.93	124.65	65.13	375.86	169.43	96.53
22500	616.23	153.85	80.37	346.84	132.16	68.07	402.12	177.23	100.03
23000	657.11	160.86	82.68	372.93	139.98	71.05	429.56	185.31	103.60
23500	699.62	168.20	85.02	400.21	148.12	74.08	458.17	193.69	107.22
24000	743.73	175.90	87.42	428.68	156.59	77.16	487.95	202.36	110.90
24500	789.44	183.97	89.86	458.32	165.39	80.28	518.88	211.34	114.65
25000	836.73	192.43	92.35	489.16	174.53	83.45	550.96	220.64	118.46
25500	885.58	201.30	94.89	521.16	184.02	86.67	584.18	230.26	122.34
26000	935.97	210.60	97.48	554.33	193.87	89.93	618.53	240.21	126.27
26500	987.89	220.34	100.13	588.66	204.08	93.23	653.99	250.51	130.27
27000	1041.31	230.55	102.83	624.13	214.67	96.57	690.55	261.15	134.34
27500	1206.20	241.23	105.60	660.74	225.63	99.95	728.18	272.15	138.47
28000	1152.56	252.42	108.43	698.46	236.98	103.37	766.88	283.51	142.66
28500	1210.33	264.12	111.32	737.29	248.71	106.83	806.62	295.23	146.93
29000	1269.52	276.36	114.29	777.21	260.85	110.33	847.38	307.33	151.25
29500	1330.08	289.15	117.32	818.20	273.38	113.87	889.15	319.80	155.65
30000	1391.98	302.51	120.43	860.24	286.32	117.44	931.89	332.66	160.11
30500	1455.21	316.46	123.62	903.32	299.67	121.04	975.59	345.91	164.63
31000	1519.73	331.00	126.89	947.41	313.43	124.68	1020.22	359.55	169.23
31500	1585.52	346.17	130.25	992.49	327.61	128.35	1065.77	373.58	173.89
32000	1652.54	361.98	133.69	1038.55	342.21	132.06	1112.20	388.01	178.61
32500	1720.76	378.43	137.23	1085.56	357.23	135.79	1159.49	402.85	183.41
33000	1790.16	395.55	140.86	1133.50	372.68	139.56	1207.62	418.20	188.27

Downloaded from <http://mnras.oxfordjournals.org/> at NASA Goddard Space Flight Ctr on July 9, 2014

Table B1 – *continued*

T (K)	Ruthenium			Rhenium			Osmium		
	Ru I ^a	Ru II ^b	Ru III ^b	Re I ^c	Re II ^d	Re III ^e	Os I ^f	Os II ^g	Os III ^h
33 500	1860.71	413.35	144.59	1182.34	388.55	143.35	1256.57	433.73	193.20
34 000	1932.37	431.85	148.42	1232.08	404.85	147.17	1306.30	449.79	198.19
34 500	2005.12	451.05	152.36	1282.68	421.58	151.02	1356.81	466.25	203.25
35 000	2078.93	470.98	156.41	1334.12	438.74	154.89	1408.05	483.13	208.38

^aRu I: experimental levels completed with HFR values as described in Fivet et al. (2009).

^bRu II–Ru III: experimental levels completed with HFR values as described in Palmeri et al. (2009).

^cCalculated using the experimental energy levels of Klinkenberg et al. (1957) with additional semi-empirical HFR values from Palmeri et al. (2006).

^dCalculated using the experimental energy levels of Meggers, Catalan & Sales (1958), Wyart (1977) and Wahlgren et al. (1997) with additional semi-empirical HFR values from Palmeri et al. (2005).

^eCalculated using the HFR energy levels predicted in this paper.

^fExperimental levels with additional HFR values taken from Quinet et al. (2006).

^gExperimental levels completed with HFR values as described in Quinet et al. (2006).

^hExperimental levels (unpublished) kindly communicated by Ryabtsev (private communication) with additional HFR values.

for $\log(\text{Pr}/N_{\text{tot}})$, which does not seem particularly useful since Pr III gives a smaller value, and the general trend is for the third spectrum of the lanthanides to give a *higher* abundance.

Neodymium [$Z = 60$; $\log(\text{Nd}/N_{\text{tot}}) = -7.03 \pm 0.32$]: the abundance is based on 12 Nd III lines. Five lines had equivalent widths over 20 mÅ, and another three were over 10 mÅ. Oscillator strengths are from DREAM.

Europium [$Z = 63$; $\log(\text{Eu}/N_{\text{tot}}) \leq -8.50$]: the upper limit is based on Eu III $\lambda 6666.37$ (Ryabchikova et al. 1999). The oscillator strength is from Wyart et al. (2008). There is no sign of a feature on the HARPS spectrum. A value of 0.4 mÅ was used to set the upper limit.

Dysprosium [$Z = 66$; $\log(\text{Dy}/N_{\text{tot}}) = -8.06 \pm 0.44$]: the abundance is based on 12 Dy III lines. All had equivalent widths ≤ 17 mÅ. Two lines gave abundances about 1 dex higher than the mean of all 12 lines. They were averaged in, but with weight 1/2. Since the logs were averaged, the difference between weighting or not weighting was only 0.1 dex. Oscillator strengths are from DREAM.

Holmium [$Z = 67$; $\log(\text{Ho}/N_{\text{tot}}) = -8.18 \pm 0.31$]: the abundance is based on 12 weak Ho III lines. Ten of the lines used were under 10 mÅ. Oscillator strengths are from DREAM.

Erbium [$Z = 68$; $\log(\text{Er}/N_{\text{tot}}) = -8.80 \pm 0.21$]: the abundance is from three Er II lines, with equivalent widths between 1.4 and 3.3 mÅ. These three are the strongest lines by far in the Reader & Corliss (1980) tabulation. Oscillator strengths are from DREAM.

Ytterbium [$\log(\text{Yb}/N_{\text{tot}}) \approx -8.69$]: the result is from Yb III $\lambda 4028.14$, $W_{\lambda} = 0.7$ mÅ. Yb II, $\lambda 4180.81$ is possibly present. $W_{\lambda} = 0.3$ mÅ, yields -9.13 . CH04 observed both Yb II and Yb III, and obtained an abundance from Yb III 0.8 dex higher than from Yb II. This is qualitatively similar to our result.

Tungsten [$Z = 74$; $\log(\text{W}/N_{\text{tot}}) \leq -8.14$]: we cannot establish the presence of W I or W II. The W II line in multiplet 1, $\lambda 3641.42$ if present is a weak feature in the wing of Ti II $\lambda 3641.33$. We estimate the equivalent width must be ≤ 0.5 mÅ. This gives an upper limit some 2.6 dex above the solar value. The oscillator strength used for $\lambda 3641$ from VALD is 0.15 dex larger than that of Kramida & Shirai (2006).

Rhenium [$Z = 75$; $\log(\text{Re}/N_{\text{tot}}) = -5.81 \pm 0.27$]: the Re II spectrum is exceptionally well developed in HD 65949, even though the strongest atomic lines of Re II are well below our wavelength coverage. Some 120 lines are attributed wholly or partially to Re II. New oscillator strengths enable us to determine abundances from lines on either side of the Balmer jump (BJ). Using 15 lines to the

violet of the BJ, we find -5.62 ± 0.21 ; 17 lines to the red of the BJ give -5.97 ± 0.22 . The sense of the difference is that the abundance of rhenium is higher in the higher atmosphere. A microturbulence of 4 km s^{-1} was necessary to remove dependence of abundance with equivalent width. This is reasonably attributed to hyperfine structure which is readily visible on the HARPS spectra. Even so, we omitted two lines with equivalent widths of 116 and 123 mÅ. The overall rhenium excess is 6 dex, which is greater than that of any element apart from mercury.

New oscillator strengths and partition functions were calculated by the Mons group. The results are presented in Tables B1 and C1.

Osmium [$Z = 76$; $\log(\text{Os}/N_{\text{tot}}) = -5.27 \pm 0.53$]: Os II is present beyond any doubt. One can see on the high-resolution HARPS spectra that the lines of Os II (and Pt II) are notably sharper than lines from lighter ions. The abundance is based on 17 lines with equivalent widths ranging from 5 to 38 mÅ. The oscillator strengths are taken from DatabasE for the SIXth Row Elements (DESIRE), and the partition functions are given in Table B1.

Platinum [$Z = 78$; $\log(\text{Pt}/N_{\text{tot}}) = -5.22 \pm 0.15$]: with Engleman's (1989) list, we identified 23 lines with Pt II. There is good evidence that the dominant isotope is ^{198}Pt (Paper I). We found no credible evidence for Pt I.

We adopt the absolute oscillator strength scale of Quinet et al. (2008, hereafter QPFB). Only three of their lines are available in HD 65949 (3535.89, 3551.36 and 4046.45 Å). Dworetzky, Storey & Jacobs (1984, hereafter DSJ) provide oscillator strengths for an additional six lines, but with a different absolute scale. The DSJ scale was based on calculated transition probabilities for UV lines that were used to fix the stellar abundance of platinum in χ Lup. Though DSJ give oscillator strengths for four lines (see their table II), in practice only two ($\lambda \lambda 1777.0$ and 2144.0) were used for the abundance which sets the astrophysical scale of DSJ's table IV. Additionally $\lambda 4046$ is in DSJ's table IV and QPFB. If we compare all four of the common UV lines, we find the DSJ $\log(gf)$ values are larger by 0.30. If we compare only the two lines used for abundance, the corresponding figure is 0.22; the DSJ $\log(gf)$ for $\lambda 4046$ is 0.42 larger than that of QPFB. We have scaled down all DSJ values by 0.30 dex. The adopted abundance is based on eight lines, not including $\lambda 4046$, which is blended with Hg I and sensitive to microturbulence and isotope shifts (Engleman 1989). Using plausible assumptions for the microturbulence, and isotope ratios, we can get good agreement from $\lambda 4046$ with results from the

Table C1. New oscillator strengths for Re II transitions. Only transitions with $\lambda > 2000 \text{ \AA}$ are included.

λ (Å)	Lower ^a	$\log gf^b$	CF ^c	λ (Å)	Lower ^a	$\log gf^b$	CF ^c	λ (Å)	Lower ^a	$\log gf^b$	CF ^c
2009.926	19 140	-0.63	0.093	2449.038	18 846	-0.44	0.198	3523.160	31 013	-2.01	0.007
2018.547	14 883	-0.87	0.139	2455.836	14 352	-0.82	0.066	3527.112	36 064	-1.76	0.014
2023.652	14 883	0.00	0.568	2467.567	14 931	-0.68	-0.140	3542.724	36 064	-1.51	-0.026
2027.206	20 463	-0.89	-0.063	2468.475	22 545	-0.95	0.041	3580.134	17 224	-0.64	0.268
2042.642	13 777	-0.83	0.099	2469.389	18 846	-0.93	0.072	3581.422	24 763	-2.17	0.005
2053.603	20 463	-0.49	-0.191	2470.610	20 463	-0.66	-0.068	3601.602	33 169	-1.95	-0.022
2055.255	14 824	-0.75	-0.113	2471.050	19 140	-0.86	-0.044	3609.339	27 746	-2.51	0.002
2059.765	14 931	-0.92	-0.044	2475.186	23 894	-0.66	-0.102	3626.781	26 237	-2.24	-0.009
2064.163	18 846	-0.81	0.102	2478.992	14 824	-0.89	0.137	3647.530	32 258	-1.55	-0.014
2075.134	19 140	-0.88	-0.040	2487.449	19 140	-0.88	0.058	3656.830	32 258	-2.07	-0.007
2075.720	14 883	-0.73	0.073	2489.028	28 095	-0.50	-0.155	3697.925	26 768	-1.79	0.031
2083.695	14 883	-0.26	0.300	2490.200	20 782	-0.42	-0.233	3714.509	30 225	-2.27	-0.005
2085.777	14 931	-0.28	-0.178	2502.350	20 976	-0.06	-0.205	3731.675	32 876	-1.61	-0.020
2091.547	20 463	-0.45	0.171	2550.086	20 463	-0.65	-0.126	3773.011	33 169	-3.51	0.000
2091.932	17 224	-0.94	-0.067	2553.525	23 894	-0.81	-0.046	3782.963	33 169	-2.31	0.005
2108.934	18 846	-0.91	-0.121	2553.604	17 224	-0.83	-0.116	3783.779	30 718	-2.43	0.003
2111.866	19 140	-0.41	0.117	2554.628	20 463	-0.18	-0.200	3791.586	29 077	-2.38	0.003
2114.251	20 976	-0.60	-0.067	2557.419	25 321	-0.91	-0.076	3800.964	18 846	-1.71	-0.128
2133.120	20 463	-0.89	0.052	2566.374	28 095	-0.64	-0.110	3823.636	37 319	-2.03	-0.014
2134.792	18 846	-0.86	-0.090	2568.636	14 883	-0.45	0.218	3826.548	31 013	-2.49	0.002
2144.083	22 545	-0.74	-0.088	2571.802	14 931	-0.64	0.221	3830.551	23 341	-1.90	-0.020
2145.896	20 463	-0.73	-0.092	2576.236	26 768	-0.80	0.059	3839.540	31 013	-1.85	-0.012
2170.806	20 463	-0.73	0.073	2588.517	29 639	-0.98	-0.046	3847.742	29 077	-2.00	-0.012
2172.108	23 146	-0.63	0.102	2588.578	20 976	-0.90	-0.106	3858.509	26 768	-2.29	0.006
2177.587	20 463	-0.85	0.063	2608.497	14 352	-0.40	0.214	3873.489	37 319	-1.89	0.026
2181.779	17 224	-0.72	0.074	2610.112	30 983	-0.89	-0.036	3915.407	37 382	-2.34	0.005
2187.911	17 224	-0.84	0.070	2610.541	25 988	-0.96	0.060	3939.368	29 773	-2.14	0.019
2190.260	14 883	-0.60	0.222	2611.537	24 763	-0.95	-0.038	3964.111	30 225	-2.06	-0.008
2195.273	20 976	-0.70	-0.081	2616.718	18 846	-0.84	-0.087	3984.242	18 846	-2.01	-0.137
2197.126	20 976	-0.91	0.050	2635.838	17 224	-0.67	0.128	4020.856	36 064	-1.65	0.028
2214.275	0	0.04	0.406	2637.006	19 140	-0.78	-0.068	4031.464	19 140	-2.11	0.041
2216.157	20 463	-0.72	0.094	2731.566	18 846	-0.68	-0.128	4032.355	32 258	-2.02	0.008
2229.106	21 629	-0.75	0.084	2733.030	17 224	-0.35	0.219	4042.758	34 937	-2.08	0.007
2247.555	20 463	-0.92	0.046	2750.551	30 983	-0.71	0.068	4089.913	26 237	-2.66	0.073
2248.627	14 931	-0.86	0.070	2813.528	30 983	-0.95	-0.078	4091.972	31 013	-1.79	-0.012
2248.763	25 321	-0.92	0.054	2875.720	28 095	-0.94	-0.060	4120.373	32 876	-2.39	0.004
2261.871	18 846	-0.83	0.061	3103.166	17 224	-0.96	-0.163	4135.441	32 876	-2.06	0.009
2272.645	19 140	-0.98	0.069	3105.075	36 064	-0.93	-0.058	4152.688	29 728	-1.91	-0.024
2275.253	0	-0.04	0.402	3298.542	36 064	-1.84	0.009	4236.149	29 077	-2.54	0.004
2286.614	19 140	-0.74	-0.058	3299.805	24 763	-1.77	0.016	4240.174	30 225	-3.09	0.002
2295.214	25 321	-0.18	0.251	3303.213	14 883	-0.95	0.123	4299.903	29 427	-2.09	0.023
2298.100	20 782	-0.12	0.278	3317.743	22 545	-1.64	0.021	4311.697	32 258	-1.97	0.009
2301.603	23 894	-0.97	0.031	3318.789	25 321	-1.07	0.072	4330.674	30 718	-1.82	-0.024
2301.805	20 976	-0.78	0.094	3331.309	37 319	-1.12	0.054	4356.283	29 728	-2.41	0.006
2303.985	23 341	-0.64	-0.116	3338.574	30 983	-1.07	-0.080	4380.967	30 983	-2.00	0.027
2308.444	20 976	-0.78	-0.125	3360.876	33 169	-2.67	-0.002	4409.547	26 768	-2.43	0.010
2324.430	23 722	-0.87	0.105	3365.390	26 666	-2.23	0.007	4422.999	22 545	-2.16	0.025
2336.928	21 629	-0.46	-0.128	3379.078	14 352	-1.09	0.170	4452.657	30 225	-2.06	-0.012
2360.297	23 894	-0.74	-0.070	3395.649	30 225	-2.01	0.006	4481.343	21 629	-2.07	-0.024
2368.563	23 894	-0.56	0.098	3403.707	30 225	-1.33	0.031	4520.959	34 937	-1.98	-0.011
2370.765	14 883	-0.84	0.098	3407.780	23 341	-1.77	-0.019	4584.473	23 341	-2.50	-0.006
2373.461	14 931	-0.95	-0.042	3411.501	27 746	-2.29	-0.003	4904.356	24 763	-2.49	0.006
2378.510	27 746	-0.88	0.042	3427.961	30 225	-2.72	-0.002	4909.738	29 077	-2.48	0.012
2382.075	24 763	-0.73	0.092	3433.839	14 824	-1.96	-0.081	5286.696	26 237	-2.83	-0.009
2386.899	20 976	-0.33	0.201	3434.898	30 225	-2.63	0.002				
2389.609	21 629	-0.89	0.058	3446.447	14 931	-1.86	-0.024				
2403.034	23 341	-0.80	0.067	3452.658	28 095	-2.22	-0.005				
2418.195	25 988	-0.33	0.127	3473.423	37 319	-1.90	0.016				
2418.394	24 763	-0.64	0.084	3485.352	30 983	-2.14	0.005				
2421.405	21 629	-0.96	-0.041	3486.190	26 768	-1.44	-0.020				
2433.732	26 237	-0.54	-0.100	3497.692	32 345	-1.99	0.010				

^aExperimental levels taken from Meggers et al. (1958), Wyart (1977) and Wahlgren et al. (1997).

^bHFR + CPOL calculations. For more details, see Palmeri et al. (2005).

^cCancellation factor as defined by Cowan (1981).

other Pt II lines. However, a definitive study of isotopes is postponed to a future study.

Gold [$Z = 79$; $\log(\text{Au}/N_{\text{tot}}) = -6.96 \pm 0.52$]: the abundance is based on Au II $\lambda\lambda 4016, 4052$ and 4361 , with equivalent widths of $4, 6$ and 3.1 mÅ. Respective abundances are $-7.17, -7.18$ and -6.11 . We have weighted the latter line $1/2$, to form the mean and standard deviation, assuming it is likely a blend. Oscillator strengths are from Rosberg & Wyart (1997).

Mercury [$Z = 80$; $\log(\text{Hg}/N_{\text{tot}}) = -4.59 \pm 0.29$]: the strength of Hg II $\lambda 3984$ is extraordinary. The abundance of mercury used here is an average of four weak Hg I and Hg II lines discussed in Papers I and II. Oscillator strengths from Fuhr & Wiese (1996) and Sansonetti & Reader (2001) cause small differences from Paper II. The uncertainty (± 0.29) is the difference of the averages: Hg II minus Hg I.

Lead [$Z = 82$; $\log(\text{Pb}/N_{\text{tot}}) \leq -8.12$]: there is no evidence for the strongest lines of either Pb I or Pb II. The upper limit used here assumes an equivalent width of 0.2 mÅ for Pb II $\lambda 5042$. If $\log(\text{Pb}/N_{\text{tot}})$ were as large as -6.0 , $\lambda 5042$ would have an equivalent width of some 16 mÅ, and be easily detected. It is clear that lead is significantly lower in abundance than osmium, platinum or mercury.

Bismuth [$Z = 83$; $\log(\text{Bi}/N_{\text{tot}}) = -8.0 \pm 0.5$]: an upper limit is from the strongest lines, $\lambda\lambda 4079$ and 5209 , discussed by Dolk, Litzén & Wahlgren (2002) for HR 7775. There is broad, weak absorption near the position of the $\lambda 5209$ components, but the Bi II hfs components do not fit it well. A measured feature, at $\lambda^* 4259.46$ is too far from the laboratory position. The upper limit is based on a synthesis that assumes a contribution from Bi II at the level of the noise.

Thorium [$Z = 90$; $\log(\text{Th}/N_{\text{tot}}) = -9.14 \pm 0.17$]: the abundance is based on eight lines with measured equivalent widths from 1.0 to 4.6 mÅ. Oscillator strengths are from DREAM. Partition functions for Th II and Th III were calculated from energy levels of Blaise & Wyart (2009). Results differ only slightly from values used at Michigan for several decades.

APPENDIX B: NEW PARTITION FUNCTIONS

Partition functions can be a significant source of error for stellar abundances if they are inaccurate. In most of this paper, partition

functions were calculated from published atomic energy levels (e.g. Moore 1949–1958), or levels produced by the Cowan (1981) atomic structure code (cf. Cowley & Barisciano 1994). This paper uses new partition functions for the first through third spectra of ruthenium, rhenium and osmium (see Table B1). These were calculated on the basis of the experimental energy levels available in the literature adding, in each case, additional theoretical values deduced from relativistic Hartree–Fock (HFR) calculations. Relevant references are indicated by footnotes to the table. Full citations appear among the main references.

APPENDIX C: TRANSITION PROBABILITIES IN RE II

Transition probabilities had been obtained by Palmeri et al. (2005) for 45 lines of Re II as a part of the general project to build the DESIRE (Fivet et al. 2007). They had used a combination of theoretical branching fractions with radiative lifetimes measured by time-resolved laser-induced fluorescence spectroscopy. The results reported were for transitions depopulating the levels with measured lifetimes. Using the same relativistic Hartree–Fock method, including core-polarization effects, the sample of results obtained by these authors has been considerably extended in this paper. More precisely, in the physical model used, the interactions between the $5d^3ns$ ($n = 6-8$), $5d^46sns$ ($n = 6-8$), $5d^6$, $5d^56d$, $5d^46s6d$, $5d^36s^26d$, $5d^46p^2$ and $5d^36s6p^2$ (even parity) and $5d^5np$ ($n = 6-8$), $5d^46snp$ ($n = 6-8$), $5d^36s^26p$ (odd parity) configurations were retained. A least-squares fit of the calculated eigenvalues of the Hamiltonian to the observed energy levels was applied, using experimental levels from Meggers et al. (1958), Wyart (1977) and Wahlgren et al. (1997). We retained 44 even-parity and 55 odd-parity levels in the fit leading to standard deviations of 135 (even) and 192 cm^{-1} (odd levels), respectively. The transition probabilities and oscillator strengths of the strongest ($\log gf > -1.0$) transitions of Re II with $\lambda > 2000 \text{ \AA}$ are reported. Additionally, lines identified wholly or partially as Re II in HD 65949 are included (see Table C1).

This paper has been typeset from a $\text{T}_{\text{E}}\text{X}/\text{L}^{\text{A}}\text{T}_{\text{E}}\text{X}$ file prepared by the author.